Hindawi
Advances in Civil Engineering
Volume 2022, Article ID 9818481, 16 pages
https://doi.org/10.1155/2022/9818481

Research Article

Model Test Study on Overburden Failure and Fracture Evolution Characteristics of Deep Stope with Variable Length

Xinfeng Wang,[1] **Youyu Wei**,[1] **Heyong Yuan**,[2] **Yiying Zhang**,[1] **Qiao Zhang**,[1] **and Wengang Liu**[1]

[1]*College of Environment and Resources, Xiangtan University, Xiangtan, Hunan 411105, China*
[2]*Department of Civil Engineering, Anhui Communications Vocational & Technical College, Hefei, Anhui 230051, China*

Correspondence should be addressed to Xinfeng Wang; wangxinfeng110@126.com

Received 10 March 2022; Revised 2 July 2022; Accepted 6 July 2022; Published 19 July 2022

Academic Editor: Qian Chen

Copyright © 2022 Xinfeng Wang et al. This is an open access article distributed under the Creative Commons Attribution License, which permits unrestricted use, distribution, and reproduction in any medium, provided the original work is properly cited.

Taking two typical stopes with variable length of working face inclined length from small to large and from large to small as the research object, the stope overburden structure model under different face length conditions is constructed through laboratory similar material simulation test, and the dynamic evolution laws of overburden instability deformation, unloading expansion, and collapse failure of forward and reverse knife handle stopes are analyzed. The three-dimensional perspective technology of parallel network electrical method is used to study the spatial distribution range and fracture development characteristics of overburden internal failure. The research shows that the overburden fracture of stope with variable length has the "time-pace-scale" evolution effect of short-time sudden change, zoning load transfer, and continuous extension. The evolution of roof fracture has experienced the development process of unloading expansion, tensile fracture instability, shrinkage deformation, and closure stability. The rise and fall of resistivity during mining in stope with variable length is closely related to the mining time step. When mining 40 cm, it is the position where the resistivity value changes suddenly. The rise of resistivity in the vertical direction makes the electric field show the transient response characteristics of dynamic expansion and rapid evolution. The development height of water conducting fracture zone of the reverse knife handle working face with the inclined length changing from large to small is slightly larger, the degree of overburden damage is high, and the fracture development is relatively sufficient.

1. Introduction

The activity of the surrounding rock in the stope is the source of the formation of mine pressure, and the appearance of the mine pressure is the specific manifestation of the activity of the surrounding rock in the stope. The root of all strata behavior in stope is the movement of upper strata caused by the mining field. Due to the differences in the surrounding rock properties, bedding structure, strength thickness, joint structure, and layer relationship of the overlying strata, the roof activity shows a variety of movement forms, and the structural characteristics of the roof determine the movement characteristics of the roof. The prevention and control concept and decision-making play a key factor [1–3], in view of the complexity and diversity of erosion rock movement, in order to comprehensively and systematically grasp the spatial failure pattern of the roof, the instability and deformation characteristics of the surrounding rock, the migration law of overlaying rock, and the characteristics of strata behavior in stope with variable length. It is necessary to conduct real-time observation and analysis on the whole process of roof fracture, roof breaking, and fracture development and evolution on the basis of profound analysis of roof spatial structure and surrounding rock characteristics [4–7]. This is important to obtain the spatial-temporal evolution law of overlying fracture field, roof displacement field, and surrounding rock fracture field, which lays a solid theoretical foundation for the study of surrounding rock control system [8–10].

Mining scholars have studied the deformation failure characteristics and dynamic response mechanism of

surrounding rock in stope with variable length. Based on the relationship between the overburden structure and the influence of large-scale breaking motion on the failure of coal and rock mass, Zhu et al. [11] studied the induced scouring mechanism of the combination mode of dynamic and static loads of the isolated island coal pillar in the irregular working face with large burial depth. Pan [12] took the occurrence principle of rock burst on the floor of all-coal roadway in the semi-isolated island working face as the research goal, established a structural model to induce underground impact pressure in the roadway, and proposed the shock initiation theory of dynamic damage of the surrounding rock of the roadway. Yang et al. [13] used the theory of overburden rock's space structure to analyze the potential area and degree of impact danger of the working face for the deeply buried irregular isolated island working face and established the use of stress online monitoring system to predict the outburst proneness of coal rock. Li et al. [7] analyzed the movement law and stress evolution characteristics of the overburden structure in the step area of the variable-length working face of Yangcheng Coal Mine. Hao et al. [14] studied the constraints and mechanical origins of dynamic disasters triggered by mining surrounding rock in the island working face with variable length and put forward the evaluation criteria for the prevention and control of shock disasters and safe and efficient mining. Around the failure characteristics of the roof surrounding rock of the coal face under different working conditions, the evolution law of the microstructure of the coal and rock mass, the distribution characteristics of the in situ stress field, and the stability control technology of the roof surrounding rock, relevant scholars have also carried out systematic research, revealing the internal mechanism of the deformation and failure of the surrounding rock of the deep stope [15–18].

To sum up, the research on the deformation, failure, and stress evolution law of surrounding rock in stope with variable length is more focused on theoretical analysis and numerical simulation, and the engineering research under experimental conditions can be used to verify the theoretical results. Laboratory similar material simulation test is a model test technology based on similarity theory. It is an important method to study natural law and solve complex engineering problems by using similarity and similar characteristics between things or phenomena. It can make up for the shortcomings of on-site monitoring and reveal the mechanical and kinematic characteristics of the simulated prototype [19–21]. Similar material simulation test is an important method to study the movement and deformation law and stress distribution characteristics of surrounding rock in the process of coal mining. With the help of physical mechanics and material science research theory, through the observation and analysis of displacement deformation, load failure, and stress-strain of the model, it can fully grasp the spatial fracture form and mechanical evolution law of stope surrounding rock [22, 23] and provide important reference value for field practice and engineering application.

2. Test Purpose and Object

2.1. Test Purpose. With the diversification of coal mining methods and the complexity of the mining environment, the working face is often affected by geological structure, folded faults, rock formation, mining conditions, and other factors, resulting in the increase or shortening of the oblique length of the working face, and mining has increased. Since most of the working faces with variable length in coal mines are mutation-type working faces, and the change mode is single, and the mining methods of multivariable working faces are relatively few. Two types of "knife-handle-style" changing face long stopes are analyzed and discussed. Through quantitative observation and qualitative research on the roof fracture shape, overlying rock migration characteristics, and crack evolution process during the mining of forward and reverse knife handle coal seams, the law of overburden deformation and failure of long stope with variable face and long stope are obtained. The evolution characteristics of fractures provide an important reference for roof management and surrounding rock prevention and control in stope with variable length.

2.2. Test Object. This similar material simulation test took the geological conditions of a stope with variable length in Huainan mining area as the research background and simulated the mining conditions of two stopes with variable length, including the forward knife handle working face and the reverse knife handle working face. The variable-length working face is 1200 m long in direction and 120–240 m long in inclination. The small plane with an inclined length of 120 m is 400 m long, and the large plane with an inclined length of 240 m is 800 m long. The advance of the working face starts from the small face to the large face, and the transition interval is the key docking area. The coal seam on this face was dominated by 13-1 coal, the total thickness of the coal seam is 3.1–5.0 m, and the average coal thickness is 3.9 m. The dip angle of the coal seam is 2–15°, the average dip angle is 7°, and the occurrence is stable. The direct roof of the working face is a composite roof composed of mudstone and 13-2 coal, with an average thickness of 3.7 m; the old roof is made of fine sandstone, with an average thickness of 10.6 m. Local fractures are developed, the connectivity and water-richness are weak, and the static storage is the main factor. The sandstone fracture aquifer on the roof of the 13-1 coal seam is the main water filling factor for this face, and it mainly enters the working face in the form of dripping water, which has little effect on the recovery. By drilling cores on the roof of the coal seam along the track 13-1 of the test working face and carrying out physic-mechanical property experiments on the rock samples taken, the mechanical parameters of the rock layers in each layer are obtained, which provides a basis for the design of model parameters.

3. Test Model Design and Monitoring Method

3.1. Design of Model Test System. This test was carried out on a three-dimensional model test platform. The three-dimensional test platform is a similar material simulation

device independently developed by the mining laboratory of Anhui University of Science and Technology, which can simulate the failure of overlying rocks in three-dimensional space. The geometric dimensions of the test platform are length × width × height = 2 m × 1 m × 2 m, and high-strength multilayer iron blocks are used to apply the load vertically. The geometric similarity ratio of the test model is 1 : 150, and the geometric size of the model is designed as length × width × height = 2 m × 1 m × 1 m, which is equivalent to the simulated stratum thickness of 150 m. Since the similar model test of the irregular stope needs to simulate the two variable-length working faces of forward knife handle, considering the size limitation of the test platform and the influence of boundary effect, the forward knife handle working face is selected. The oblique length was designed to be 80 to 160 cm, which was equivalent to the oblique length of the on-site working face of 120 to 240 m. The oblique length of the reverse knife handle working face was designed to be 80~160 cm, which was equivalent to the oblique length of the on-site working face of 120 m to 240 m. The length direction of the test platform was the oblique length direction of working face, and the width direction of the test platform was regarded as the direction of working face. The working face was pushed forward and parallel along the width direction of the platform, and 10 cm boundary coal pillars were left on both sides of the front and rear of the model to eliminate the boundary effect during mining. Protect the coal pillars to ensure normal advancement during mining at the face. The three-dimensional mining model of "knife-handle-style" variable-length working face is shown in Figure 1, and the schematic diagram of the plane model is shown in Figure 2.

According to the similarity principle and dimensional analysis requirements, combined with the lithology, bulk density, strength, and other field conditions of the roof-floor of coal seam, the similar parameters in the model are converted, and the corresponding ratio is determined. Similar materials use fine sand as aggregate, and lime and gypsum as cement. In order to accurately determine the ratio of similar materials to obtain the required parameters, a large number of standard specimens were specially selected for physical and mechanical tests, and the material ratio is adjusted through repeated tests. And finally the best ratio table of similar materials for each layer is obtained, as shown in Table 1. According to the requirements of the optimal proportion table, determine the material proportion, bulk density, layer thickness, and model size to calculate the dosage and then make a model according to the dosage requirements and sprinkle mica powder between each layer to play a layering role. In the actual model making process, because the coal seam mining of the three-dimensional model was more complicated, the coal seam can be replaced by thin wood strips of similar thickness. According to the test requirements, 8 short wood strips with a length of 80 cm, a width of 5 cm, and a thickness of 2.6 cm can be processed and made, and at the same time, 8 long wood strips with a length of 160 cm, a width of 5 cm, and a thickness of 2.6 cm can be processed and made, a total of 16 wood strips. The surrounding of the wooden strips was wrapped with transparent tape to reduce friction. During the test process, when laying on the coal seam, all thin wooden strips were used instead. At the same time, the wooden strips are slowly pulled out to implement isometric advancement, and each time a wooden strip is pulled out is equivalent to advancing 5 cm on the working face. The coal seam of the forward knife handle working face was along the model trend (i.e., width direction), which first lay 8 short wooden strips with a length of 80 cm and then lay 8 long wooden strips with a length of 160 cm. While the laying sequence of the reverse knife handle working face was on the contrary, in the coal-bearing rock layer, 8 long wooden strips with a length of 160 cm were first laid along the model direction, and then 8 short wooden strips with a length of 80 cm were laid. The position of the eighth wooden strip was the position where the oblique length of the working face changes.

3.2. Test Monitoring Method. The self-developed parallel direct current method was used to detect the abnormal space of the overlying rock damage in the forward and reverse knife handle stope, and the three-dimensional space perspective technology of the parallel electric method was used to study the spatial distribution range and fracture development status of the internal damage of the overlying rock.

The advantage of the parallel network electrical measuring instrument is that any electrode was powered, and the potential measurement can be performed on all the other electrodes at the same time, which can clearly reflect the natural potential of the detection area and the change of the primary power field potential, and the data acquisition efficiency is greatly improved. According to the different forms of power supply, the data acquisition methods of parallel electrical method are divided into monopole powered AM method and dipole powered ABM method. The layout of AM method is the same as that of the secondary method, and the potential is collected as a single point. When one electrode supplies power, the electrode is a pole, and the remaining electrode is m pole for potential data collection. For the data collected by this method, the resistivity data of two pole and three pole devices can be extracted for inversion through postprocessing, and at the same time, high-density electrical detection can be realized. ABM electrical data acquisition is powered by dipoles; that is, two electrodes A and B are powered at the same time, without using infinite electrodes, and only a reference electrode n is set near the instrument. The data collected by this method include all the data required by all quadrupole devices. It can obtain the data measured by all kinds of quadrupole arrangement devices through one measurement, which greatly improves the collection efficiency, and the data measured by the electrodes are synchronous, which reduces the error of the collection system. For example, when 64 electrodes were arranged on the measuring line, when the AM method was used for acquisition, during the power supply of any electrode, the remaining 63 electrodes simultaneously collected the potential, so that the data acquisition efficiency was at least 63 times higher than that of

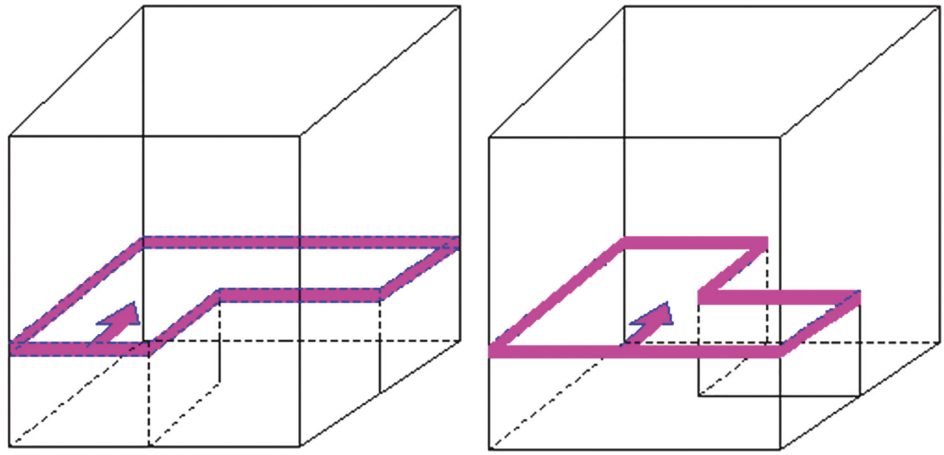

(a) (b)

Figure 1: The three-dimensional mining model of working face with variable length. (a) Forward knife handle working face. (b) Reverse knife handle working face.

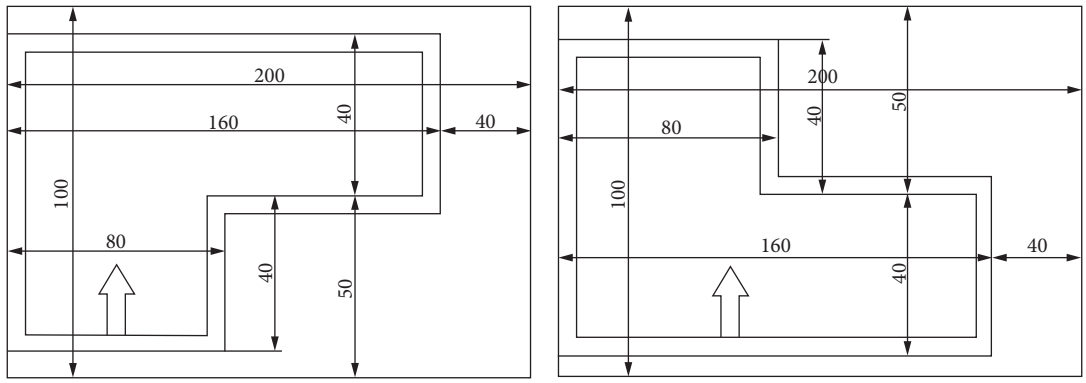

(a) (b)

Figure 2: Plane model diagram of working face with variable length (unit: cm). (a) Forward knife handle working face. (b) Reverse knife handle working face.

the series acquisition. Moreover, the AM method and ABM method were used to automatically switch the electrodes in order to obtain a large number of electrical data, which can not only decompile all the data detected by the current DC high-density resistivity method but also realize the inversion of high resolution resistivity method, and good monitoring results were achieved. During observation period, the AM method data acquisition was performed using the electrode system in a single borehole, and the electrode current data were used for inversion. In order to highlight the change effect, a unified icon was used for the current ratio result image, and cold and warm tones of different colors are used to represent the degree of current change.

The experiment adopts the method of laying two layers of electrodes to collect and analyze the three-dimensional electric field spatial data. The electrode of the first layer was laid 15 cm above the coal seam of the test model, and the actual control failure height of the overlying rock was 22.5 m. Then a total of 48 electrodes were arranged, and the distance between adjacent electrodes was 3 cm. It was divided into two sides, and 24 electrodes are arranged on each side. The specific size layout was shown in Figure 3(a). The electrode of the second layer was laid at a position 40 cm above the coal seam of the test model, and the actual control failure height of the overlying rock was 60 m. A total of 64 electrodes are arranged on the second layer, and the electrode spacing was 3 cm. It was also divided into two sides, and 32 electrodes are arranged on each side. The specific size layout was shown in Figure 3(b).

The two tests were conducted over a total of 10 days, with each test lasting for 5 days, including the installation of the test system, background value testing, data acquisition during mining, postmining stability observations, and dismantling of the observation system. The data were decompiled, dedistorted, and exported using AGI's Earth-Imager 3D software. The electrode position 1# of the 2 layers above the coal seam was taken as the coordinate origin (0, 0, 0), and the model was taken to the right as the positive x-axis direction, inwards as the positive z-axis direction and downwards as the positive z-axis direction to establish a 3D three-dimensional spatial coordinate system, as shown in Figure 4.

Table 1: The comparison table of the field conditions of working face and simulation parameter.

Rock name	Prototype parameters			Model parameter				
	Thickness (m)	Compressive strength (MPa)	Volumetric weight (kg/m^3)	Thickness (cm)	Compressive strength (MPa)	Volumetric weight (kg/m^3)	Material ratio	Water ratio
Gravel stratum	16.3	140.13	2894	10.9	0.78	1608	9 : 0.5 : 0.5	1/10
Sandy mudstone	21.9	21.06	2538	14.6	0.12	1410	8 : 0.7 : 0.3	1/10
Medium sandstone	2.1	137.68	3390	1.4	0.76	1883	5 : 0.6 : 0.4	1/10
Spotted mudstone	10.2	34.72	2568	6.8	0.19	1427	9 : 0.7 : 0.3	1/10
Medium sandstone	3.2	129.60	3410	2.1	0.72	1894	5 : 0.6 : 0.4	1/10
Sandy mudstone	14.7	20.89	2507	9.8	0.12	1393	8 : 0.7 : 0.3	1/10
Fine sandstone	9.2	113.85	3143	6.1	0.63	1746	6 : 0.6 : 0.4	1/10
Sandy mudstone	9.4	27.53	2564	6.3	0.15	1425	8 : 0.7 : 0.3	1/10
Fine sandstone	10.3	108.62	2920	6.9	0.60	1622	6 : 0.6 : 0.4	1/10
Sandy mudstone	2.1	30.59	2550	1.4	0.18	1417	8 : 0.7 : 0.3	1/10
Sandstone	1.6	91.24	2815	1.1	0.51	1564	5 : 0.6 : 0.4	1/10
Shale	1.8	41.73	2595	1.2	0.23	1442	7 : 0.7 : 0.3	1/10
13-1 coal seam	3.9	8.2	1326	2.6	0.05	737	10 : 0.5 : 0.5	1/10
Mudstone	4.1	28.24	2638	2.7	0.16	1465	7 : 0.7 : 0.3	1/10
Sandy mudstone	7.2	27.89	2520	4.8	0.15	1400	8 : 0.7 : 0.3	1/10
Medium sandstone	16.1	141.76	3426	10.7	0.79	1903	5 : 0.6 : 0.4	1/10
Mudstone	15.0	29.62	2530	10.0	0.17	1406	8 : 0.7 : 0.3	1/10

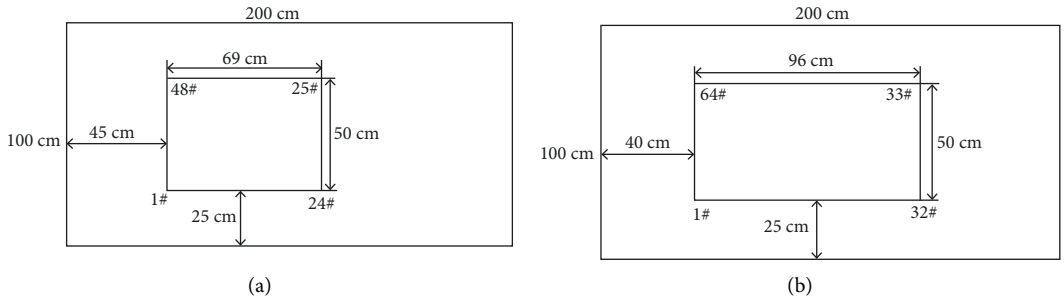

Figure 3: The physical model of electrical test system layout. (a) 15 cm above the coal seam and (b) 40 cm above the coal seam.

4. Characteristics of External Damage and Fracture Distribution in the Overburden of Long Variable Face Quarries

By analyzing the evolution of overburden caving failure during the mining process of the forward and reverse knife handle working face, the potential law of roof breaking and fracture development distribution characteristics of stope with variable length can be obtained. Figures 5 and 6 specifically reflected the external forms of rock failure in two types of stope with knife handle. The working face starts to move forward from the opening of incision, and when it advanced to about 30m, some of the rock formations collapsed and collapsed instantaneously after the first pressure directly on the top, and the shape of the rock formations after the collapse is relatively broken (Figure 6(a)). When the working face is continued to advance to 60 m, the immediate roof completely collapsed, forming an irregular caving zone. The main roof began to break and collapsed in a step-down manner. During this period, cracks began to derive and develop, breaking cracks appeared above the caving zone and continued to develop to the deep level, and separated cracks formed between the strata sinking in the stage (Figures 5(b) and 6(b)). Then with the progress of coal seam mining activities, when the working face is advanced to 90 m, the main roof continued to fall in stages from bottom to top, and its fracture characteristics showed staged features. The ruptured fractures developed rapidly, and the abscission fractures expand gradually and dynamically forward, and the two fractures form fracture derivative zone in the upper space of the overlying rock (Figures 5(c) and 6(c)). Then, when the working face is advanced to 120 m, the main roof is broken periodically, part of the rock layers below the goaf is recompacted, and the fracture development

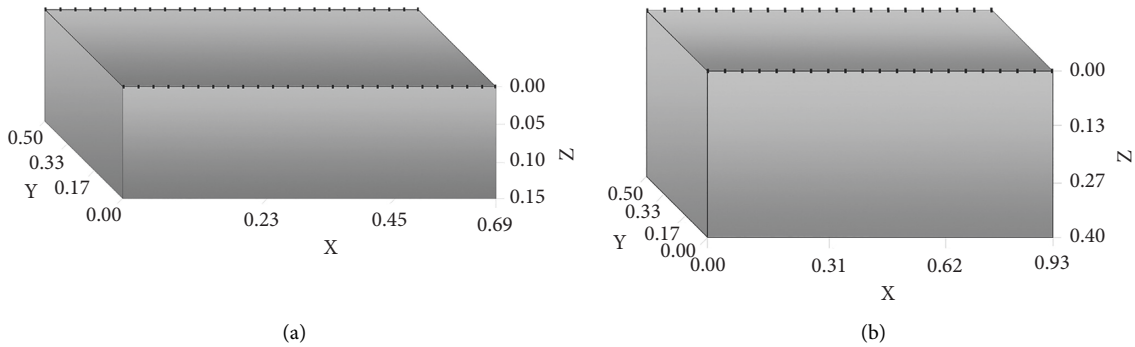

Figure 4: The three-dimensional space coordinate system in the different layers of the model. (a) 15 cm above the coal seam and (b) 40 cm above the coal seam.

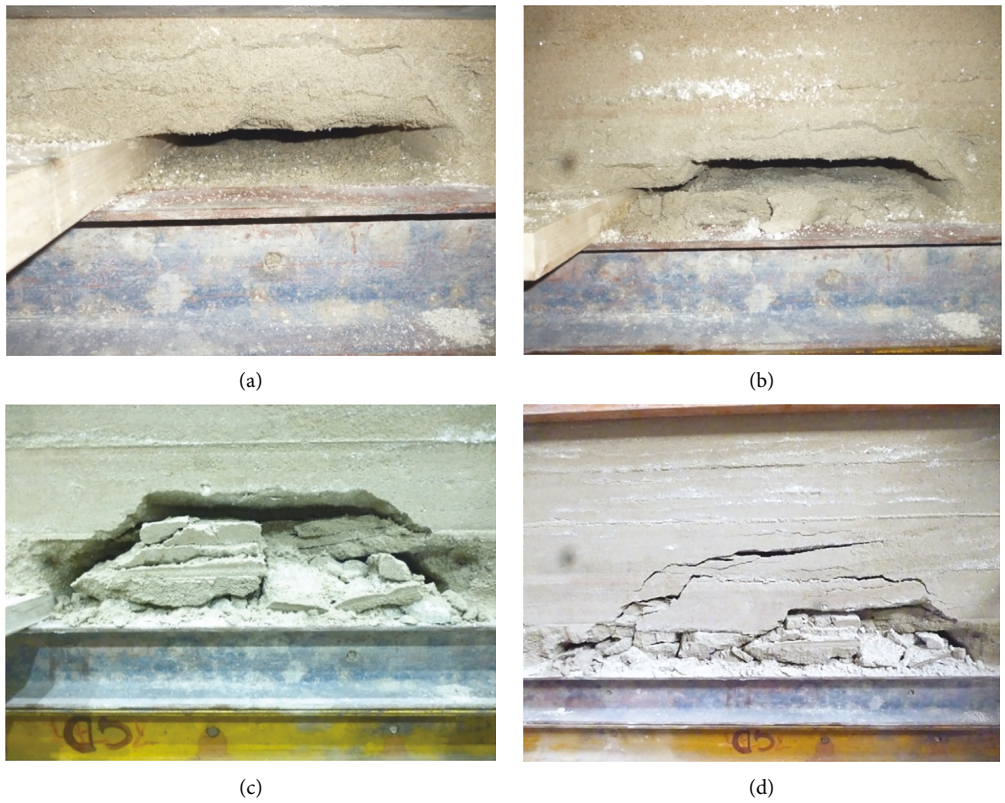

Figure 5: External failure form of overlying rock in forward knife handle working face. (a) Mining 30 m. (b) Mining 60 m. (c) Mining 90 m. (d) Mining 120 m.

space is extended to the high level. Nearby interlayer fissures are clearly developed (Figures 5(d) and 6(d)).

Looking at the process of the external overburden destruction of the two types of "knife-handle-type" stope with variable length, it can be found that the damage degree of the roof during the mining period of the forward knife handle working face was lower than that of the reverse knife handle working face. The failure strength of weathered rock weakened, and the roof-caving form is relatively regular. The development time of weathered rock fissures is slightly lagging behind, and the expansion space of transverse fissures is relatively small. According to the comprehensive analysis, the deformation and failure of surrounding rock continuously develop forward and upward in the process of the two types of variable-length working faces, and there are periodic fractures and collapses. The roof fracture has the temporal and spatial characteristics of instantaneous suddenly change, subsection extension, and subregional migration. The overlying rock fracture field has undergone a dynamic evolution process of pressure relief and instability, tension fracture failure, shrinking, and fitting and sealing. Its expansion space is trapezoidal to the depth developing.

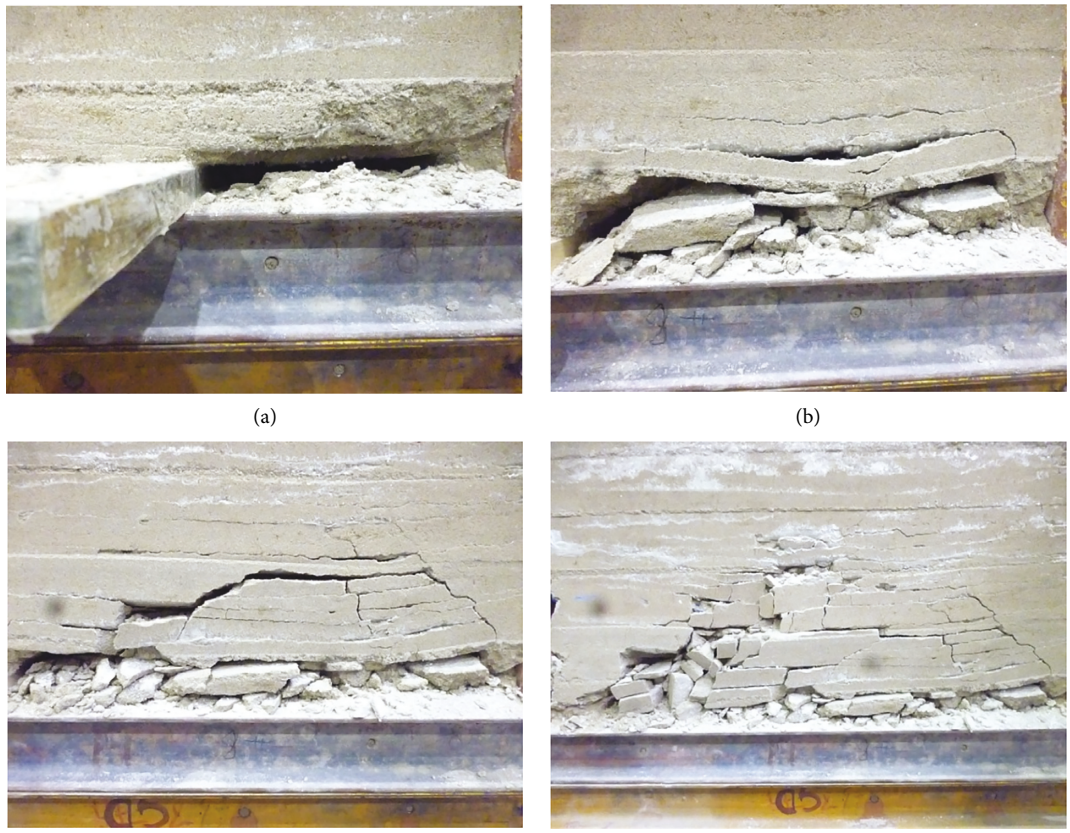

(a) (b) (c) (d)

Figure 6: External failure form of overlying rock in reverse knife handle working face. (a) Mining 30 m. (b) Mining 60 m. (c) Mining 90 m. (d) Mining 120 m.

5. Internal Failure and Crack Evolution Characteristics of Overlying Rock in Stope with Variable Length

In order to analyze and judge the damage law of the overlaying rock and temporal evolution of the fracture development in the internal three-dimensional space of the forward and reverse knife handle of two types of stope with variable length, the parallel electrical test technology is used on the site to test the various coal seam mining. Dynamic evolution characteristics of the distribution of fractures in the overlying rock are revealed through specific graphs such as resistivity three-dimensional inversion map, resistivity dynamic cross section map, resistivity slice map, and resistivity slice ratio map. The resistivity change is affected by many factors, such as hydrogeological conditions, the layered characteristics of surrounding rock, lithological characteristics, excavation disturbance and damage characteristics, stress distribution changes, displacement and deformation, and fracture evolution. It has the characteristics of sensitive response, high accuracy, timely detection response, and so on. With the help of the effective results of resistivity data monitoring, the two zone failure height in the three-dimensional space inside the overburden can be accurately determined and comprehensively evaluated.

5.1. The Internal Destruction and Fracture Development Characteristics of the Overlying Rock in the Forward Knife Handle Stope

5.1.1. Stereo Inversion Image of Resistivity. Figure 7 reflects the variation trend of the three-dimensional spatial resistivity of the overlying rock 15 cm above the coal seam of the forward knife handle working face. It can be found in the figure that the coal seam is in the mining interval of 20~60 cm, and the resistivity changes obviously. When the coal seam is advanced to 40 cm, the resistivity changed abruptly, and the increasing trend of resistivity showed a large difference in the z-axis direction. The difference in resistivity is the specific manifestation of different damage degrees inside the overlying rock, and the rise and fall of the resistivity affect the development and distribution space of the overlying fissures. Therefore, the distribution boundary of the two zones of overlying rock can be judged according to the difference of resistivity. According to the image analysis, the height of the caving zone is about −0.05 m.

Figure 8 is three-dimensional spatial resistivity inversion image of overlying rock at a position 40 cm above the coal seam of the forward knife handle working face, reflecting the electrical variability characteristics of the overlying surrounding rocks at internal rock mass space in multiple

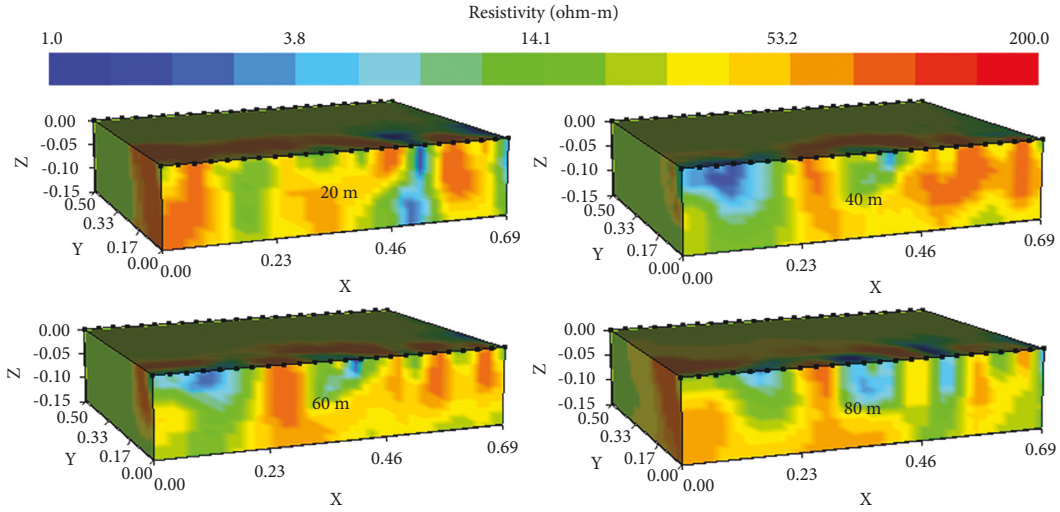

Figure 7: Three-dimensional resistivity inversion map of strata at 15 cm above the coal seam.

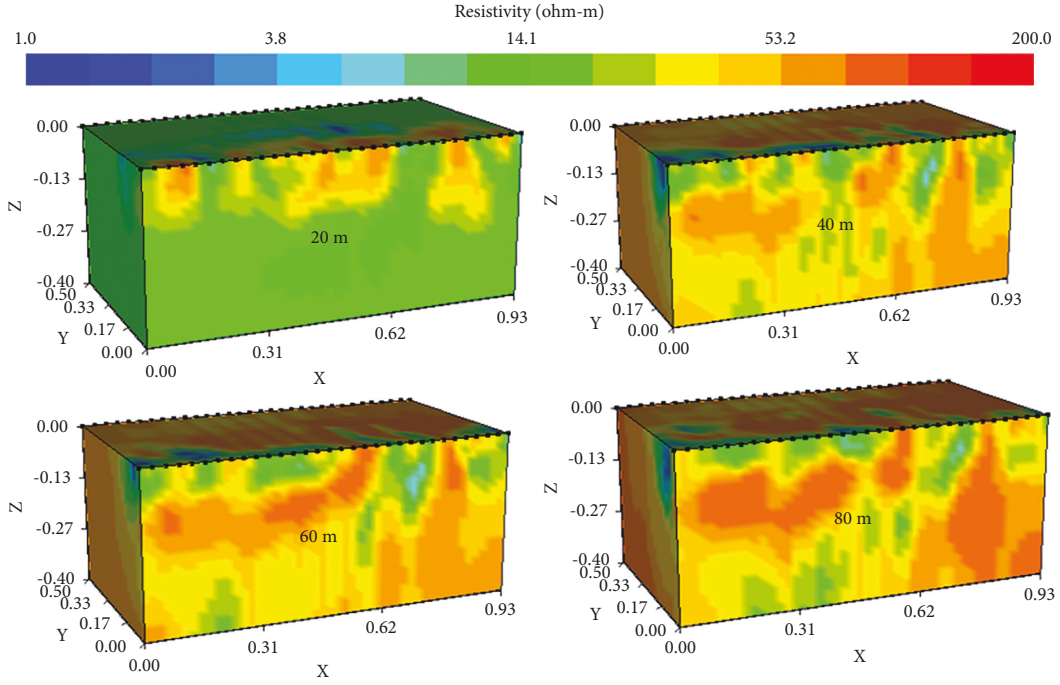

Figure 8: Three-dimensional resistivity inversion map of strata at 40 cm above the coal seam.

mining stages under the test of the second layer observation system. The change of resistivity can be seen directly from the figure, and the resistivity of the three-dimensional space surface background value before working face mining is relatively low. With the gradual increase of the mining degree of the working face, the resistivity increases, and the increase trend is fast. When the working face is advanced to 40 cm and enters the working face contact area, the high resistivity range expands and the cracks develop obviously, indicating that the overlying rock collapses at this stage. At the end of the working face mining, the height of the increase in resistivity in the observation space reaches −0.11 m. Judged from the comprehensive evolution process of resistivity, the coal seam mining has an obvious change trend of resistivity in the range of 15–20 cm before and after the but joint, and this range is also the main active interval for overlying rock damage and fracture development.

5.1.2. Dynamic Evolution Process of Resistivity. Figures 9 and 10 are the internal multiangle cross-sectional views of the electric field in the three-dimensional space of the overlying rock at different layers above the coal seam of the forward knife handle working face, which can clearly reflect the

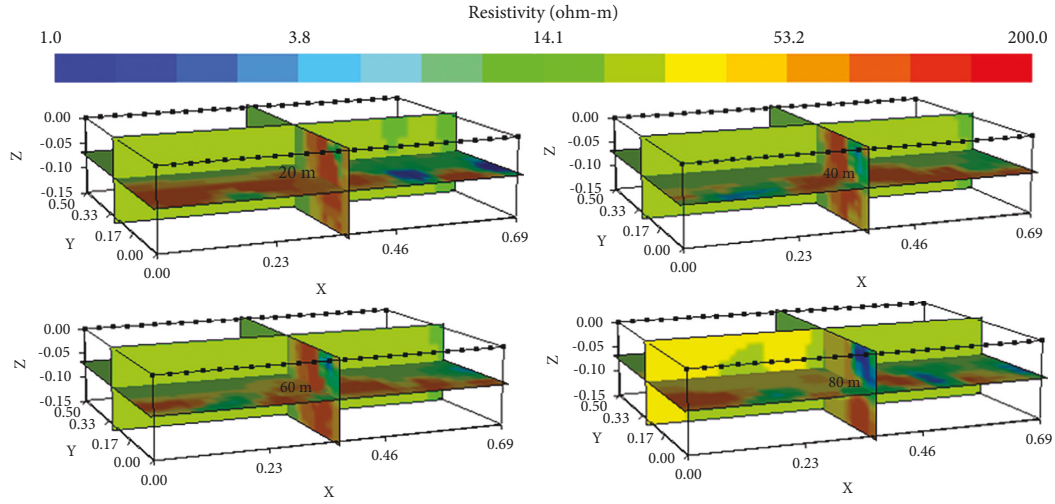

Figure 9: The resistivity section diagram of dynamic at 15 cm above the coal seam.

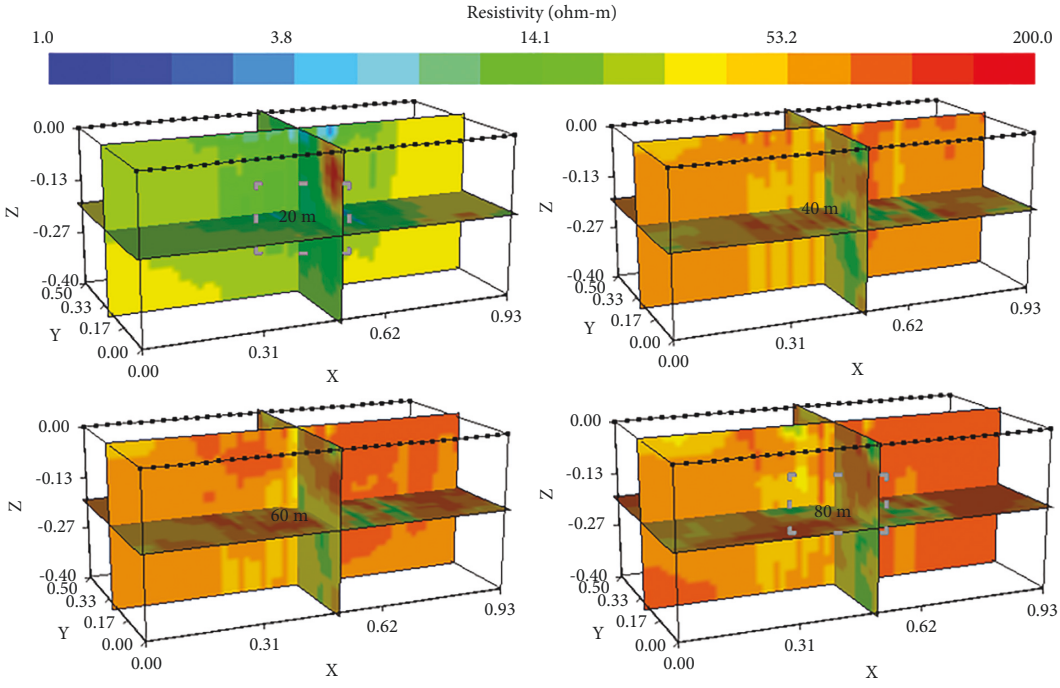

Figure 10: The resistivity section diagram of dynamic at 40 cm above the coal seam.

electric field response characteristics of each mining stage in the rock formation space inside the model.

According to the analysis in Figures 9 and 10, the resistivity value was small before the test starts, and the maximum resistivity reached 200 Ω·m at the end of the test.

The 40 cm stage of coal seam mining is the time point when the electric field fluctuates the most. At this time, the resistivity value changes greatly after the coal seam mining, and the resistivity value also changes to varying degrees in the space around the mining. When the working face is advanced to 60 cm, due to the expansion of the length, the overburden resistivity of increase area of 15 cm above the coal seam is extended to the position at 69 cm in the x-axis direction. The overburden resistivity of increase area of 40 cm above the coal seam is extended to the spatial position at 90 cm in the x-axis direction. The location where the resistivity value changes abruptly is the rapidly developing section of abscission fractures. The derivative development of vertical interlayer fractures accelerates the morphological evolution of the resistivity from irregular scattered points to strip-shaped blocks, showing a dynamic expansion spatio-temporal response features.

5.1.3. Resistivity Slice Map. Figures 11 and 12 are the slice images of the resistivity of the overlying rock at different layers above the coal seam in the forward knife handle stope at 7 different positions along the x-axis direction, and the

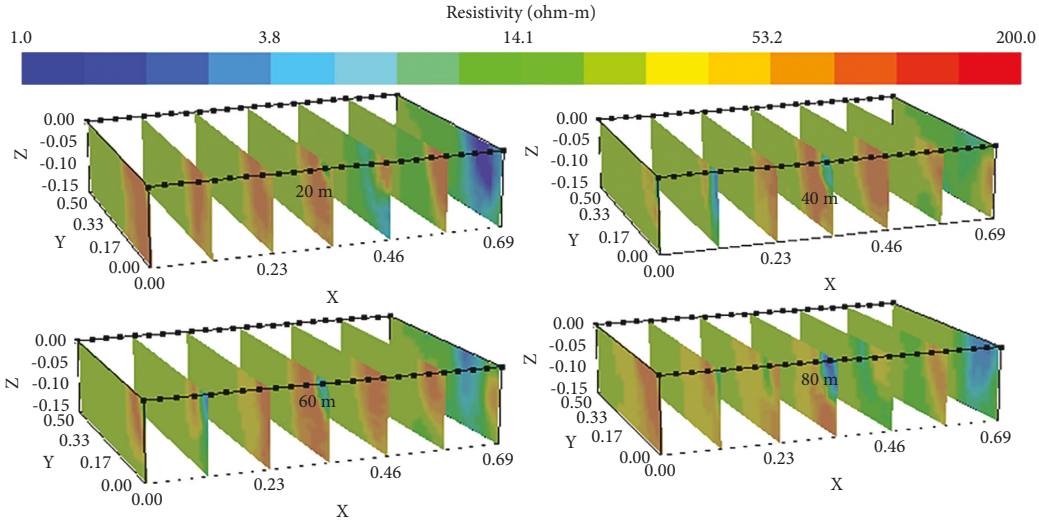

Figure 11: The resistivity section diagram along the x-axis direction at 15 cm above the coal seam.

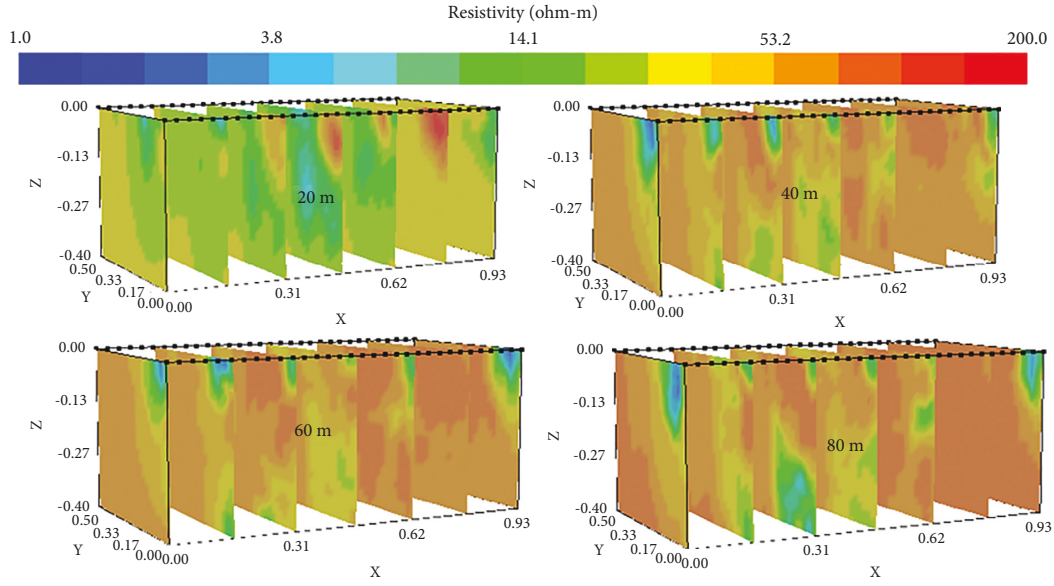

Figure 12: The resistivity section diagram along the x-axis direction at 40 cm above the coal seam.

damage height and dynamic changes of the overlying rock in different mining stages of the coal seam can be visually observed feature. It can be seen from the resistivity slice diagrams in Figures 11 and 12 that the area where the resistivity first changes is in the part with a smaller scale value in the y-axis direction, and the overlying rock failure height also follows this law, which fully conforms to the characteristics of rock failure resistivity increase caused by coal seam mining. The change interval of the rapid increase of resistivity is located in the mining stage of 20~60 cm, and the change of electrical characteristics is an intuitive reflection of the rupture of the internal structure of the rock stratum.

5.1.4. Resistivity Slice Ratio Diagram. Figures 13 and 14 are the ratios of the x-z plane resistivity of $y = 26$ cm to the background before mining in multiple mining stages of the forward knife handle working face. It can be found that from the figure that when the working face is advanced to 20 cm, the resistivity of x-z plane remains unchanged. When the working face is advanced to 40 cm, the resistivity above 0.2~0.42 m in the x direction increases significantly.

When the working face is advanced to 60 cm, the overlaying rock above the position of 0.5~0.65 m in the x-axis direction is damaged greatly. After the mining of the

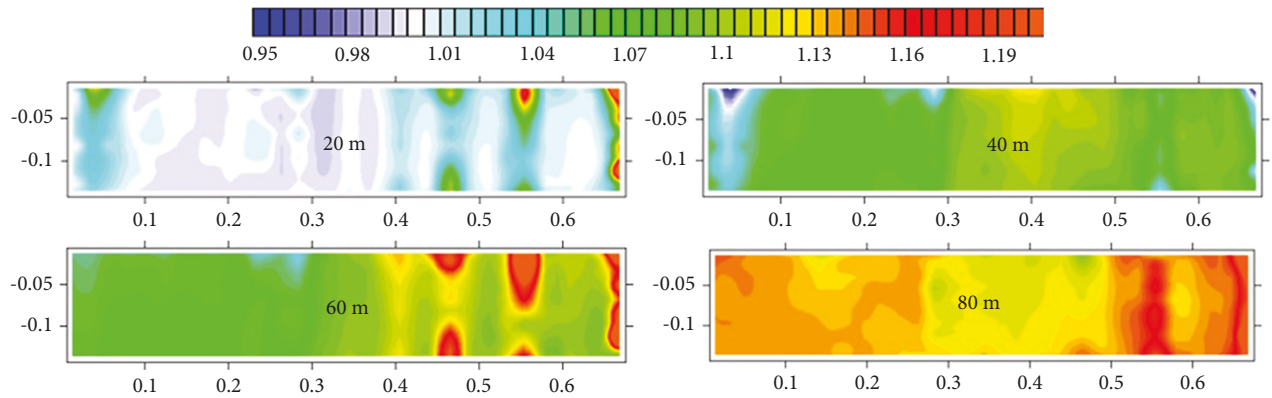

Figure 13: The resistivity section ratio chart in the x-z plane at 15 cm above the coal seam ($y = 26$ cm).

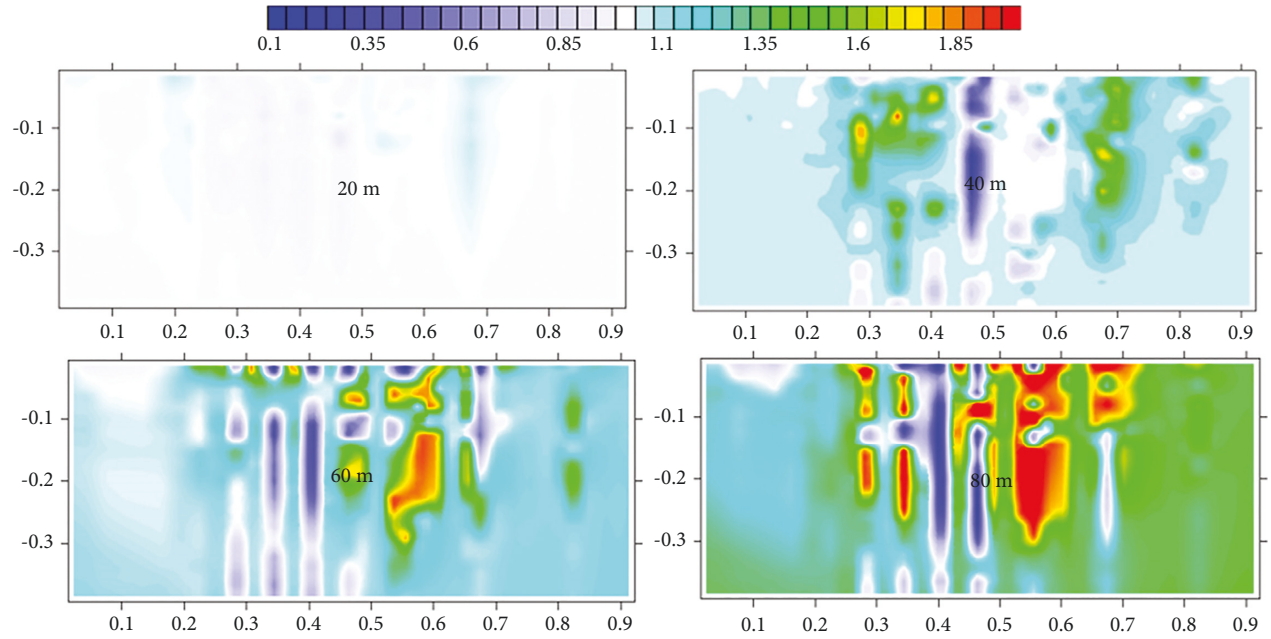

Figure 14: The resistivity section ratio chart in the x-z surface at 40 cm above the coal seam ($y = 26$ cm).

working face is completed, the overburden failure height is roughly in the range of –0.1 m.

5.2. The Internal Damage and Fracture Development Characteristics of Overlying Rock in the Reverse Knife Handle Stope

5.2.1. Stereoscopic Inversion Image of Resistivity. Figures 15 and 16 are three-dimensional spatial resistivity stereo inversion images of the overlying rock at 15 cm and 40 cm above the coal seam of the reverse knife handle working face, which intuitively reflect the three-dimensional resistivity variation characteristics of the roof in each mining stage. The resistivity of the background value in the inner three-dimensional space of the working face before mining was relatively low, the resistivity value began to increase after the mining of 20 cm, and the surface electric field in the three-dimensional space showed cloud-like distribution characteristics. When the working face is advanced to 40 cm, the range of resistivity elevation zone increases, the electrical properties of the rock formation show great differences in the z-axis direction, and the distribution space of the electric field in the three-dimensional space expands accordingly. After working face is advanced to 60 cm, the resistivity still maintains a rapid growth momentum, and the interlayer fractures develop and expand to a great extent. When the working face is advanced to 80 cm, the height of the increase of resistivity in the observation space reaches –0.12 m, and the failure height of the overlying caving zone is –0.07 m. In the range of 20 cm before and after the butt-joint mining, the resistivity changes obviously, and this range is also the key activity range for overlying rock damage and fracture development.

5.2.2. Dynamic Evolution Process of Resistivity. Figures 17 and 18 show the internal multiangle cross-sectional views of the three-dimensional electric field of the overlying rock at different layers above the coal seam of the

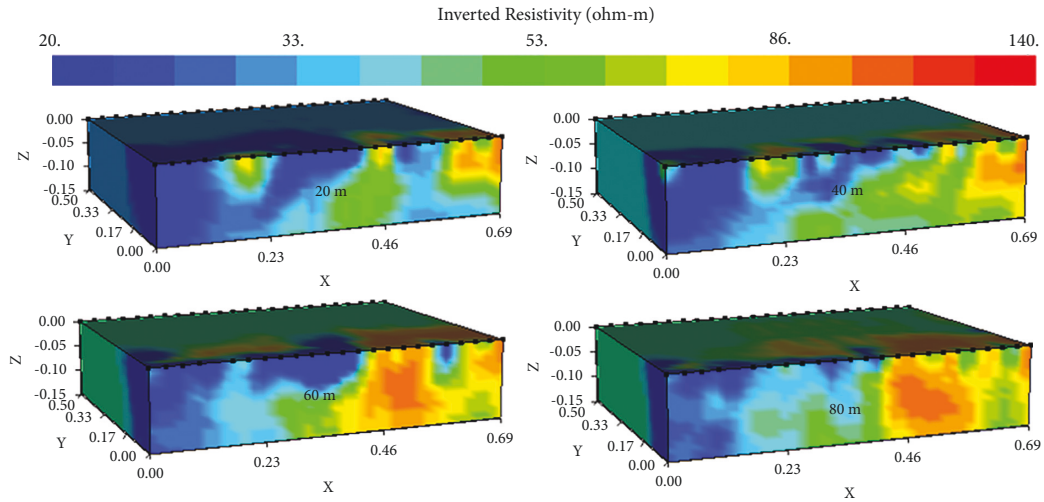

Figure 15: Three-dimensional resistivity inversion map of strata at 15 cm above the coal seam.

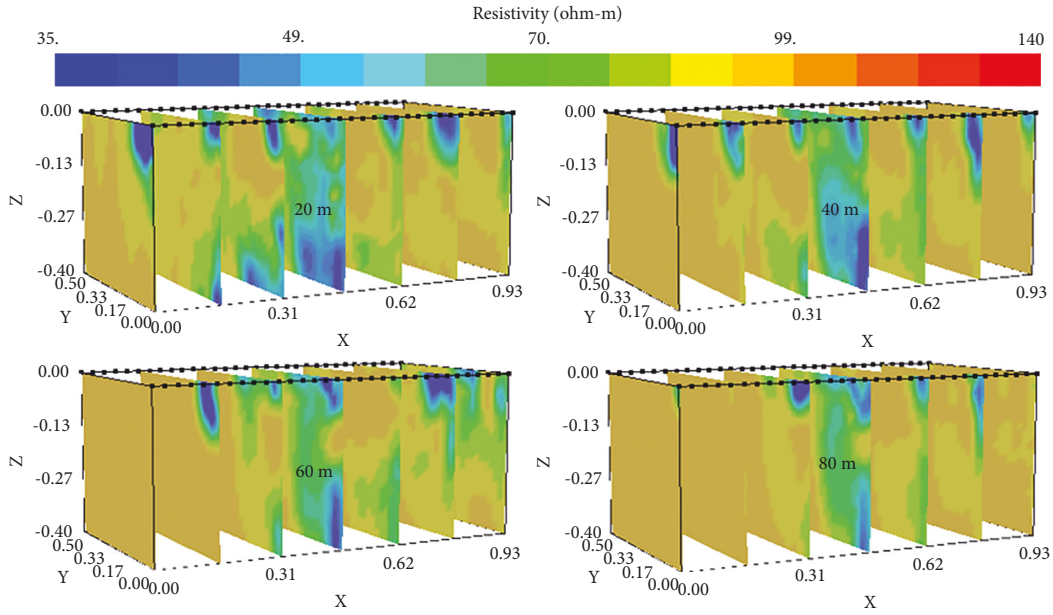

Figure 16: Three-dimensional resistivity inversion map of strata at 40 cm above the coal seam.

reverse knife handle working face, which better reveals the electric field response characteristics of the rock space in the model at different mining stages. Figures 17 and 18, which better reveal the electric field response characteristics of the rock formation space inside the model at different mining stages. The resistivity value of coal seam before mining is relatively small, and the maximum resistivity after mining is as high as 220 Ω·m, an increase of nearly 5 times. The 30~50 cm range of working face mining is the time period when the electric field fluctuates the most. At this time, the space resistivity values behind and around the coal seam mining were changed to a great extent. After 60 cm of working face mining, the increased resistivity of overlying rock in the first horizon above the coal seam extends to 65 cm in the x-axis direction, and the increased resistivity of overlying rock in the second horizon extends to 93 cm in the x-axis direction. During the mining process of working face, the location where the resistivity value changes abruptly is usually the hardest hit area of overlying rock damage. The layer damage of overlying rock leads to the rapid development of interlayer cracks, which makes the electric field show the characteristics of dynamic expansion and rapid evolution of transient response.

5.2.3. Resistivity Slice Diagram. Figures 19 and 20 are slice images of resistivity at 15 cm and 40 cm above the coal seam of reverse knife handle working face at seven different positions along the x-axis, which can intuitively reflect the development height of two zones of failure field and the dynamic evolution characteristics of roof fracture field in different mining stages. Similar to the electric field evolution

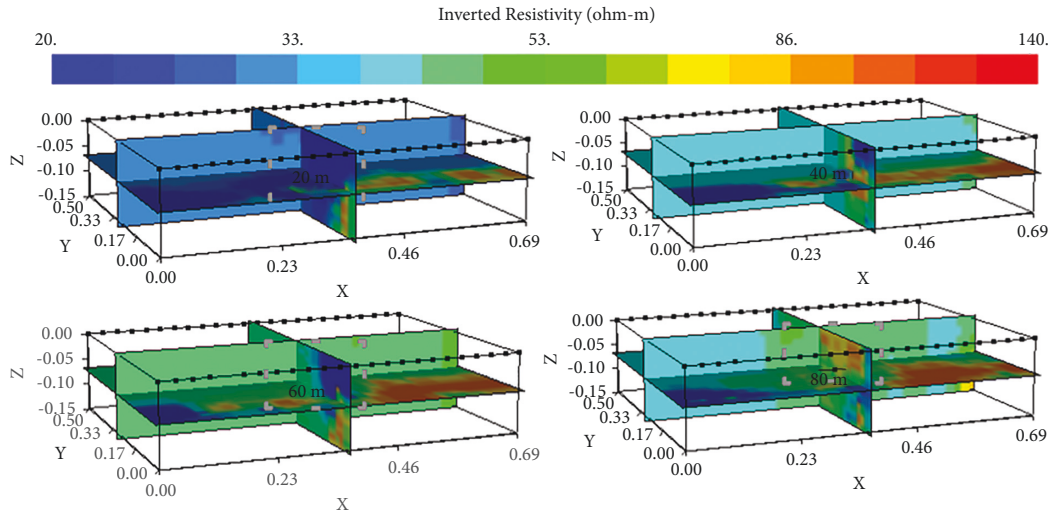

Figure 17: The resistivity section diagram of dynamic at 15 cm above the coal seam.

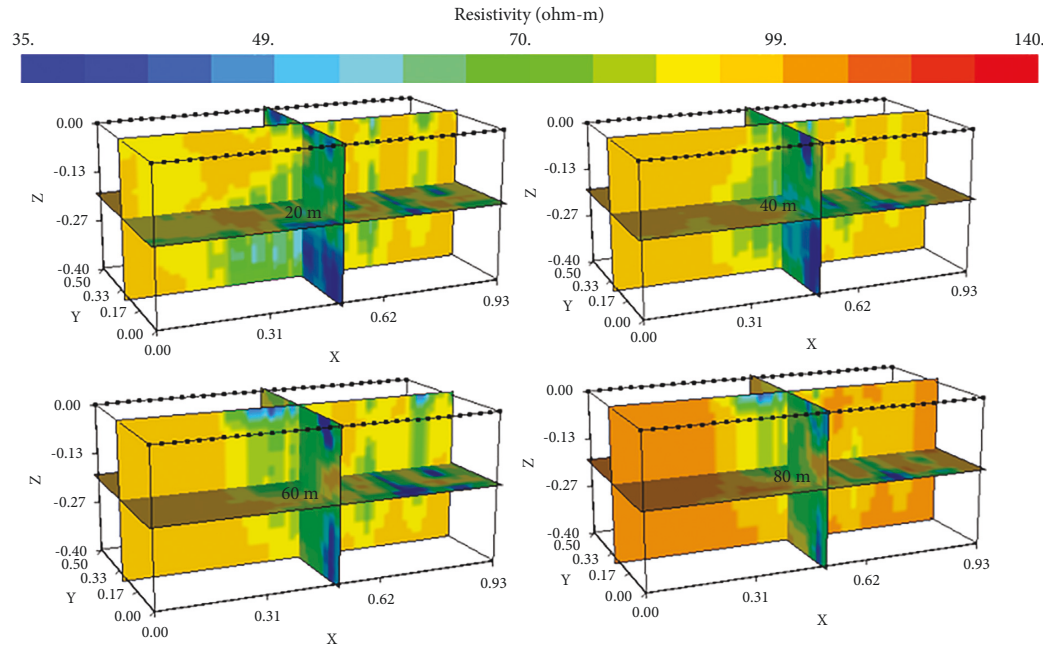

Figure 18: The resistivity section diagram of dynamic at 40 cm above the coal seam.

process of the forward knife handle working face, the area where the resistivity first changes is located in the area where the scale value is small in the y-axis direction, and the electrical characteristics in this change range have changed. The change of resistivity is correlated with the mining time step, which fully conforms to the law of the increase of resistivity caused by the destruction of strata caused by coal seam mining. The drastic change period of resistivity growth is located in the mining interval of about 20 cm before and after the contact area of working face. The change of electrical characteristics in this stage will induce the deformation, dislocation, and concentrated fracture of the internal structure of the rock stratum.

5.2.4. Resistivity Slice Ratio Diagram. Figures 21 and 22 show the ratios of the x-z plane resistivity of $y = 26$ cm to the background before mining in multiple mining stages of the reverse knife handle working face. When the working face is advanced to 20 cm, the resistivity value of the x-z planes changes locally, but the overall change is not obvious. When the working face is advanced to 40 cm, the resistivity of the position above 0.26–0.52 m in the x-axis direction increases significantly; after the working face is advanced to 60 cm, the overlying rock above the position 0.45–0.63 m in the x-axis direction is damaged greatly. After the mining of the working face is completed, the overburden failure height is roughly in the range of −0.15 m. Judging from the ratio of

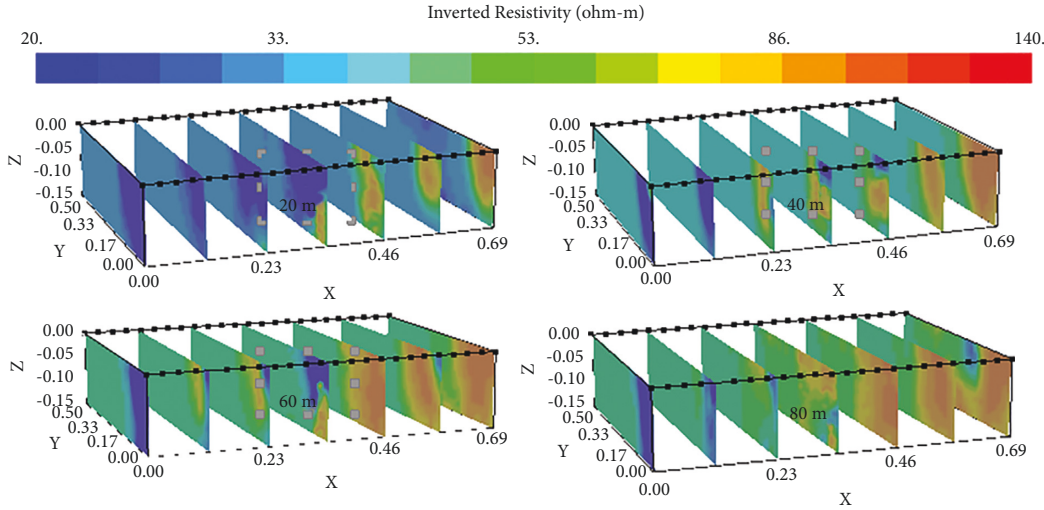

Figure 19: The resistivity section diagram along the x-axis direction at 15 cm above the coal seam.

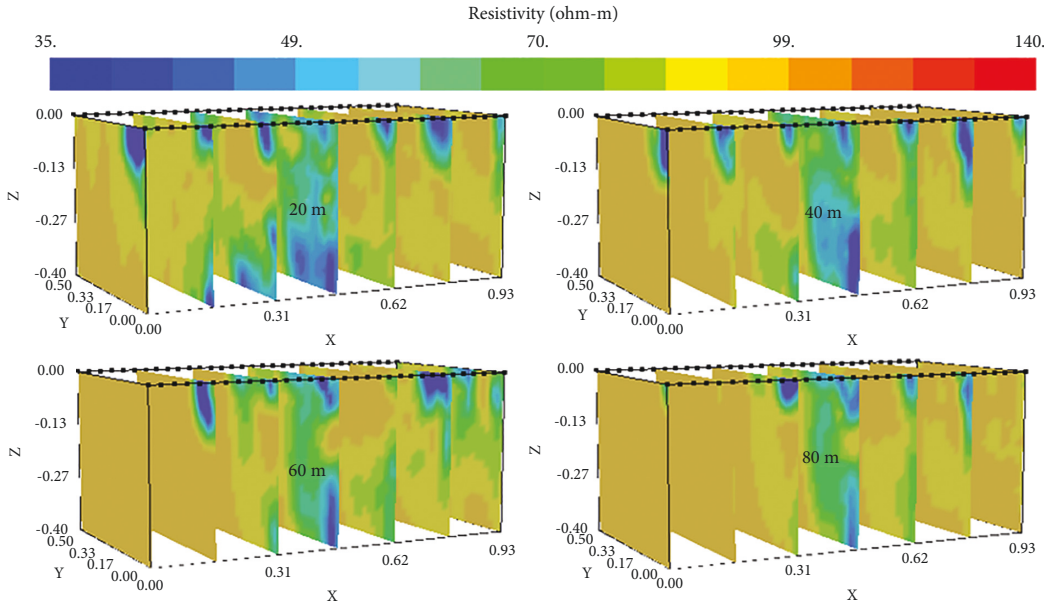

Figure 20: The resistivity section diagram along the x-axis direction at 40 cm above the coal seam.

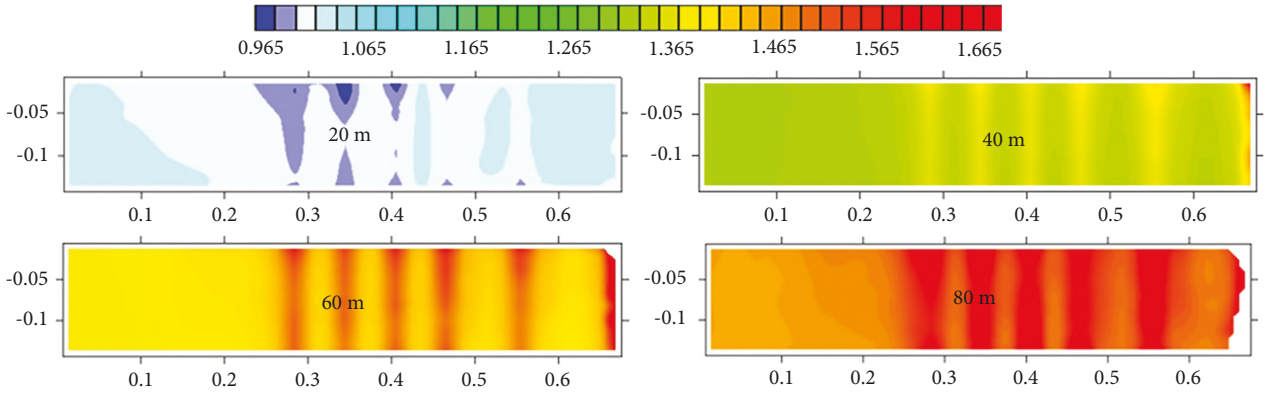

Figure 21: The resistivity section ratio chart in the x-z plane at 15 cm above the coal seam ($y = 26$ cm).

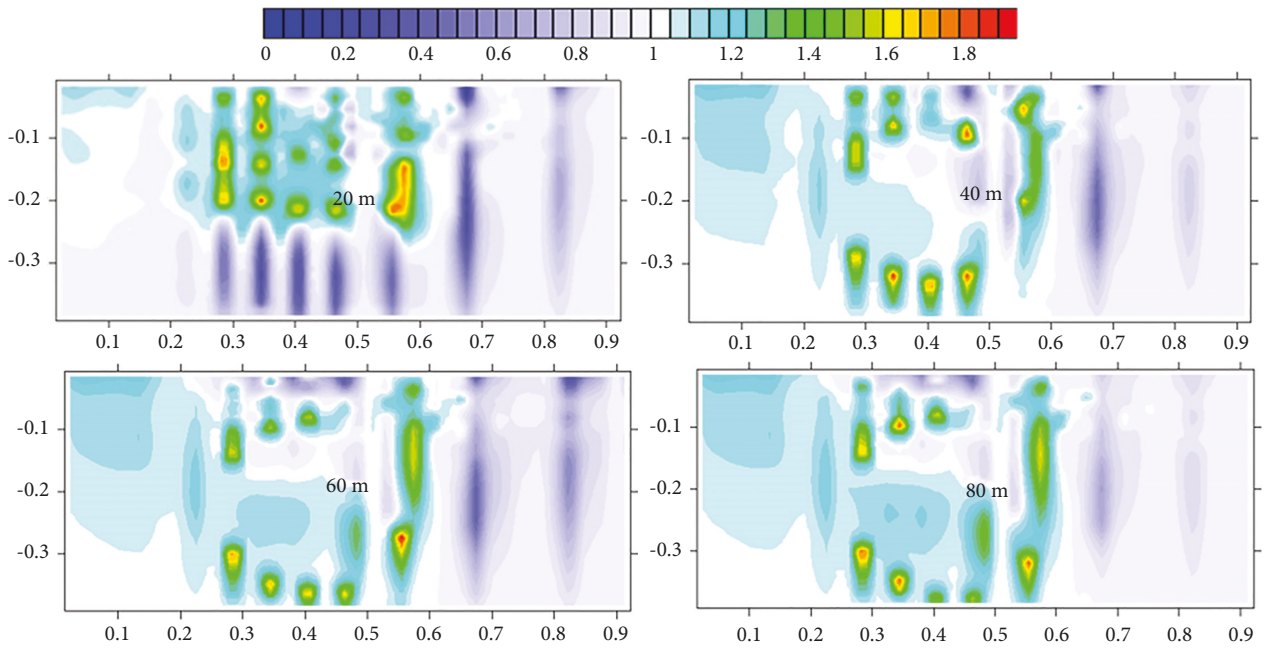

Figure 22: The resistivity section ratio chart in the x-z plane at 40 cm above the coal seam ($y = 26$ cm).

resistivity slices at 15 cm and 40 cm above the coal seam of the working face, the resistivity variation area of the second horizon is significantly higher than that of the first horizon. The electrical characteristics are more significant, and the expansion space of the electric field dynamic response is more extensive.

6. Conclusions

(1) Roof fracture during the mining of stope with variable length has the characteristics of mutation, regionality, and ductility. The evolution of the overlying fissure field is from pressure relief instability to tension fracture failure, then shrinking and finally fitting and sealing. The fracture expansion space is trapezoidal, from shallow to deep and from near to far. Roof damage degree of the forward knife handle stope during mining is lower than that of the reverse knife handle stope, the damage strength of the overlying rock is weakened, and roof-caving pattern is relatively regular; the development time of the overlying cracks is slightly delayed, and the expansion space of transverse cracks is relatively small.

(2) The rise and fall of resistivity during the advancing process of "knife-handle-style" working face are closely related to the mining time step. The sharp change period of the resistivity growth of the two types of stope is located in the mining interval within 20 cm of contact area before and after working face. The change of electrical characteristics in this stage will induce the deformation, dislocation, and concentrated fracture of the internal structure of the rock stratum. At 40 cm, the resistivity value changed abruptly. The increasing trend of resistivity shows a big difference in the z-axis direction, which prompt the electric field to show the transient response characteristics of dynamic expansion and rapid evolution.

(3) Compared with the reverse knife handle working face, the height of caving zone of the former is about 10 cm, corresponding to the actual height of 15m. The height of the fissure zone is about 30 cm, corresponding to the actual height of 45 m. The height of the later is about 12 cm, corresponding to the actual height of 18 m. Height of the fissure zone is 35 cm, corresponding to the actual height of 52.5 m. The development height of the two zones of the forward knife handle working face is slightly larger, the degree of damage to the overlying rock is higher, and the development of fissures is relatively sufficient.

(4) In this paper, the mechanical evolution characteristics of roof deformation and instability, load transfer, stress evolution, and collapse failure of two typical variable face length stopes with variable face length from small to large and from large to small are studied by using laboratory similar material simulation test and parallel network electrical method three-dimensional perspective technology. In the later stage, the engineering verification will be carried out in combination with the existing theoretical analysis and model test results to further deepen the research on relevant topics.

Data Availability

The data used to support the findings of this study are included within the article.

Conflicts of Interest

The authors declare that they have no conflicts of interest regarding the publication of this paper.

Acknowledgments

This work was supported by the National Natural Science Foundation of China (Grant no. 51904266), Excellent Youth Project of Hunan Provincial Department of Education (Grant no. 21B0144), and 2022 Funding Project for Young Backbone Teachers in Colleges and Universities in Hunan Province and Research Project on Teaching Reform of Colleges and Universities in Hunan Province in 2020 (Grant no. HNJG-2020-0231).

References

[1] X. F. Wang, M. Y. Lu, and Y. H. Gao, "Structural mechanical characteristics and instability law of roof key block breaking in gob side roadway," *Advances in Civil Engineering*, vol. 2020, Article ID 6682303, 2020.

[2] G. R. Feng and P. F. Wang, "Stress environment of entry driven along gob-side through numerical simulation incorporating the angle of break," *International Journal of Mining Science and Technology*, vol. 30, pp. 189–196, 2018.

[3] C. J. Hou, X. Y. Wang, and J. B. Bai, "Basic theory and technology study of stability control for surrounding rock in deep roadway," *Journal of China University of Mining & Technology*, vol. 50, no. 01, pp. 1–12, 2021.

[4] H. Wu, B. Dai, L. Lu, R. Zhao, G. Liang, and W. Liang, "Experimental study of dynamic mechanical response and energy dissipation of rock having a circular opening under impact loading," *Mining, Metallurgy & Exploration*, vol. 38, no. 2, pp. 1111–1124, 2021.

[5] X. F. Wang, *Slope Length Effect of Roof Fracture Mechanism and Stress Distribution Characteristics of Irregular Stope*, AnHui University of Science and Technology, Huainan, 2015.

[6] B. W. Lu, C. W. Liu, and H. Xie, "Law of overburden strata movement and mining roadway deformation under mining influence in the unequal length of working face," *Metal Mine*, vol. 01, pp. 34–38, 2016.

[7] Y. Y. Li, S. C. Zhang, and L. Q. Gao, "Mechanism and prevention of pressure burst in step region based on overburden strata movement of unequal length working face," *Rock and Soil Mechanics*, vol. 37, no. 11, pp. 3283–3290, 2016.

[8] Y. G. Wang, W. B. Guo, and E. H. Bai, "Characteristics and mechanism of overlying strata movement due to high-intensity mining," *Journal of China Coal Society*, vol. 43, pp. 28–35, 2018.

[9] D. D. Chen, F. L. He, and S. R. Xie, "Time-space relationship between periodic fracture of plate structure of main roof and rebound in whole region with elastic foundation boundary," *Chinese Journal of Rock Mechanics and Engineering*, vol. 38, no. 06, pp. 1172–1187, 2019.

[10] X. F. Wang, M. Z. Gao, and Y. X. Chen, "Analysis of Fracturing Characteristics of stope roof based on elastic thin plate theory," *Metal Mine*, vol. 06, pp. 24–28, 2015.

[11] G. A. Zhu, L. M. Dou, and Y. Liu, "Rock burst mechanism analysis on deep irregular island face," *Journal of Mining & Safety Engineering*, vol. 33, no. 04, pp. 630–635, 2016.

[12] J. F. Pan, "Start-up principium of rock burst in whole coal roadway floor in half-island face," *Journal of China Coal Society*, vol. 36, pp. 332–338, 2011.

[13] G. Y. Yang, F. X. Jiang, and C. W. Wang, "Prevention and control technology of mine pressure bumping of coal mining face in seam island based on deep mining and thick topsoil of complex spatial structure of overlying strata," *Chinese Journal of Geotechnical Engineering*, vol. 36, no. 01, pp. 189–194, 2014.

[14] J. Hao, M. W. Xu, and W. B. Wu, "Study on the prevention and control of dynamic disasters at an isolated island working face," *China Earthquake Engineering Journal*, vol. 39, no. 05, pp. 976–980, 2017.

[15] X. Li, Z. Xu, and Y. Xu, "Characteristics and trends of coal mine safety development," *Energy Sources, Part A: Recovery, Utilization, and Environmental Effects*, vol. 2020, no. 12, 19 pages, Article ID 1852339, 2020.

[16] S. Liu, X. Li, D. Wang, and D. Zhang, "Investigations on the mechanism of the microstructural evolution of different coal ranks under liquid nitrogen cold soaking," *Energy Sources, Part A: Recovery, Utilization, and Environmental Effects*, vol. 2020, no. 07, 17 pages, Article ID 1841856, 2020.

[17] X. L. Li, S. J. Chen, S. M. Liu, and Z. H. Li, "AE waveform characteristics of rock mass under uniaxial loading based on Hilbert-Huang transform," *Journal of Central South University*, vol. 28, no. 6, pp. 1843–1856, 2021.

[18] P. Guo, X. Zhang, Y. Peng, M. He, C. Ma, and D. Sun, "Research on deformation characteristic and stability control of surrounding rock during gob-side entry retaining," *Geotechnical & Geological Engineering*, vol. 38, no. 3, pp. 2887–2902, 2020.

[19] X. J. Zhu, G. L. Guo, and J. F. Cha, "Optical image method to deformation monitoring of similar material model," *Journal of China University of Mining & Technology*, vol. 44, no. 01, pp. 176–182, 2015.

[20] H. C. Li, *Similar Simulation Test of Mine Pressure*, Journal of China University of Mining & Technology, China, 1988.

[21] D. Z. Kong, Y. Xiong, and Z. Cheng, "Stability analysis of coal face based on coal face-support-roof system in steeply inclined coal seam," *Geomech. Eng*, vol. 25, no. 03, pp. 233–243, 2021.

[22] Y. Xue, T. Teng, and X. H. Wang, "Analysis of fracturing model and caving law of stope roof," *Science Technology and Engineering*, vol. 16, no. 07, pp. 156–161, 2016.

[23] F. L. He, W. R. He, and D. D. Chen, "First fracture structure characteristics of main roof plate considering elastic-plastic deformation of coal," *Journal of China Coal Society*, vol. 45, no. 08, pp. 2704–2717, 2020.